Impact of charge-coupled device size on axial measurement error in digital holographic system

Hao, Yan; Asundi, Anand Krishna

2013

Hao, Y., & Asundi, A. K. (2013). Impact of charge-coupled device size on axial measurement error in digital holographic system. Optics letters, 38(8), 1194-1196.

https://hdl.handle.net/10356/96318

https://doi.org/10.1364/OL.38.001194

Impact of charge-coupled device size on axial measurement error in digital holographic system

Yan Hao[1,*] and Anand Asundi[2]

[1]*Department of Instrument Science and Engineering, Shanghai Jiaotong University, Shanghai 200242, China*

[2]*School of Mechanical and Aerospace Engineering, Nanyang Technological University, Singapore 639798*

**Corresponding author: ya0001ao@e.ntu.edu.sg*

Received November 26, 2012; revised February 21, 2013; accepted February 26, 2013;
posted February 26, 2013 (Doc. ID 179905); published April 1, 2013

Digital holography (DH) is a 3D measurement technique with a theoretical axial resolution of better than 1–2 nm. However, practically, the axial resolution has been quoted to be in the range 10–20 nm. One possible reason is that the axial measurement error is much larger so that the theoretical axial resolution cannot be achieved. Until now the axial measurement errors of the DH system have not been thoroughly discussed. In this Letter, the impact of CCD chip size on the axial measurement error is investigated through both simulation and experiment. The results show that a larger CCD size reduces the axial measurement error and improves the measurement accuracy of edges.

OCIS codes: 090.0090, 090.1995.

Digital holography (DH) [1,2] is a 3D measurement technique. As lateral (x and y directions) and axial (z direction) measurements are based on different mechanisms, DH has different lateral and axial resolution capabilities. The lateral resolution is limited by the diffraction effect and cannot go beyond submicrometer level. The axial measurement is based on measurement of the optical path differences (OPDs). One quantity that limits OPD measurement is the quantization effect [3]. For an 8 bit system, this limits the resolution to about 2 nm. Thus the axial resolution is much better than the lateral resolution. Hence much more effort has been put into investigation of lateral rather than axial resolution in the DH system [4–7]. However, in practical applications, the theoretical axial resolution cannot be achieved [8–11]. One possible reason is that other factors, such as pixel size and CCD size, also contribute to axial resolution. These have not been investigated much until now. In this Letter, the impact of CCD size on the axial measurement errors of the practical DH system is investigated.

In the DH system, the reconstructed wavefront $Rf(x)$ of an object $f(x)$ can be expressed, according to the diffraction theory, as

$$\begin{aligned} Rf(x) = \text{Fresnel}\Bigg[\Bigg(\Bigg\{\Bigg[f(x) \otimes \exp\left(\frac{j\pi}{\lambda z}x^2\right)\Bigg] \\ \times \exp(-j2\pi a x) \times \text{rect}\left(\frac{x}{2D}\right)\Bigg\} \otimes \text{rect}\left(\frac{x}{2p}\right)\Bigg) \\ \times \exp(j2\pi a x) \times \sum_{-\infty}^{+\infty} \delta(x - nS)\Bigg], \end{aligned} \tag{1}$$

where $\otimes$ denotes convolution. The operator denotes the Fresnel transform [12]. λ, z, and a are the wavelength, the distance between the object and the CCD plane, and the carrier frequency introduced by the off-axis reference wave, respectively. $2D$, $2p$, and S are the CCD chip size, the pixel sensing size, and the CCD sampling interval, respectively. x represents the coordinate in the object plane, the CCD plane, and the image plane. Due to the separable property of Fresnel transformation, without loss of generality, a 1D case is considered.

In Eq. (1), the first convolution describes the propagation of the object wave from the object plane to the CCD plane. At the CCD plane, the interference with the reference wave $\exp(-j2\pi a x)$ gives rise to two first-order diffraction spectrums. One of these spectrums, corresponding to the wavefront $\{f(x) \otimes \exp[j\pi x^2/(\lambda z)]\} \times \exp(-j2\pi a x)$ in space, is used in the reconstruction step. Factors $\text{rect}\{x/(2D)\}$, $\text{rect}\{x/(2p)\}$, $\exp(j2\pi a x)$, and $\sum_{-\infty}^{+\infty} \delta(x - nS)$ correspond to the finite CCD size, the pixel integration effect, the compensation of the reference wave tilt, and the CCD sampling effect, respectively. According to the convolution theorem of the Fourier transform, Eq. (1) can be rewritten as

$$Rf(x) = R_0 f(x) * \sum_{n=-\infty}^{\infty} \delta\left(x - \frac{n\lambda z}{S}\right) \tag{2}$$

with

$$\begin{aligned} R_0 f(x) = \text{Fresnel}\Bigg[\Bigg(\Bigg\{\Bigg[f(x) \otimes \exp\left(\frac{j\pi}{\lambda z}x^2\right)\Bigg] \\ \times \exp(-j2\pi a x) \times \text{rect}\left(\frac{x}{2D}\right)\Bigg\} \otimes \text{rect}\left(\frac{x}{2p}\right)\Bigg) \\ \times \exp(j2\pi a x)\Bigg]. \end{aligned} \tag{3}$$

Equations (2) and (3) show that the sampling effect generates multiple replicas of image $R_0 f(x)$ with an interval of $(\lambda z)/S$. Usually only one replica $R_0 f(x)$ is used for measurement. The sampling effect does not affect the measurement in cases where the replicas do not overlap. Therefore $R_0 f(x)$ is used to investigate the impact of CCD size on the axial measurement in this Letter. A similar model was presented in [6] without consideration of the reference wave and its conjugate. In [6], the

point spread function (PSF) of an arbitrary point source at x_0 can be expressed by the Fresnel transform of $\mathrm{sinc}[2p/(\lambda z)\times(x-x_0)]\times\exp[j\pi/(\lambda z)\times(x-x_0)^2]\times\mathrm{rect}[x/(2D)]$. By following the same analysis process but including the reference wave and its conjugate, the PSF of Eq. (3) can be derived as the Fresnel transform of $\mathrm{sinc}[2p/(\lambda z)\times(x-x_0-\lambda z a)]\times\exp[j\pi/(\lambda z)\times(x-x_0)^2]\times\mathrm{rect}[x/(2D)]$. Expanding the above Fresnel transform gives the PSF of an arbitrary point at x_0 as

$$\mathrm{PSF}(x)=\exp\left[-\frac{j\pi}{\lambda z}(x^2-x_0^2)\right]\times\left\{\left[\exp\left(j2\pi\frac{x_0+\lambda z a}{\lambda z}x\right)\times\mathrm{rect}\left(\frac{x}{2p}\right)\right]\otimes\mathrm{sinc}\left(\frac{2D}{\lambda z}x\right)\otimes\delta(x-x_0)\right\}. \quad (4)$$

The PSF in Eq. (4) is influenced by the interaction of terms $2D$, $2p$, a, and x_0. The PSF in Eq. (4) is used to facilitate the analysis in the later part of this Letter.

To analyze the impact of the finite CCD size on the axial measurement error, a simulation based on Eq. (3) is performed first. In the simulation, the object step height is shown as the red solid line corresponding to an OPD of 100 nm (Fig. 1). The width of the substrate is 297.6 μm on either side of the step whose width is 595.2 μm. In the simulation, λ, z, and S are 633 nm, 139.91 mm, and 4.65 μm, respectively. The reconstructed OPD is shown by the blue dotted line in Fig. 1. The OPD errors of the reconstructed image can be easily noticed. The edges are not sharp and the ringing around the edges of the object is severe. Three factors are used to define the OPD errors. The first is the maximum OPD error (MOE) of the step, which is the average of the two MOEs located at the positions indicated by the two black dotted lines. The second is the averaged OPD error (AOE) of the step. The third is the edge width (EW), which is the width between the MOE point on the step and the MOE point on the substrate indicated by the two green arrows.

The impact of finite CCD size on OPD error is investigated with CCD size $2D$ varying from 2.3808 to 16.666 mm in steps of 2.3808 mm. The following values are used: $2p=S=4.65$ μm and $a=53.76\times10^3$ Hz. The object is symmetrically located with respect to the optical axis. Figure 2 illustrates the dependence of MOE, AOE, and EW on the CCD size. Figures 2(a) and 2(b) show that a larger CCD size reduces the OPD error. From

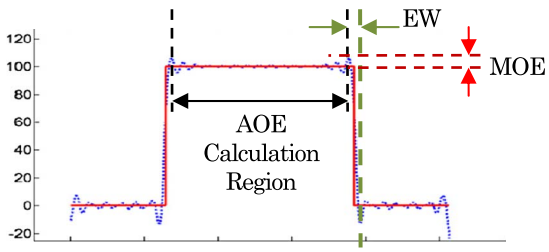

Fig. 1. (Color online) OPD profile of a step object (red solid line) and an example of its reconstructed OPD image (blue dotted line).

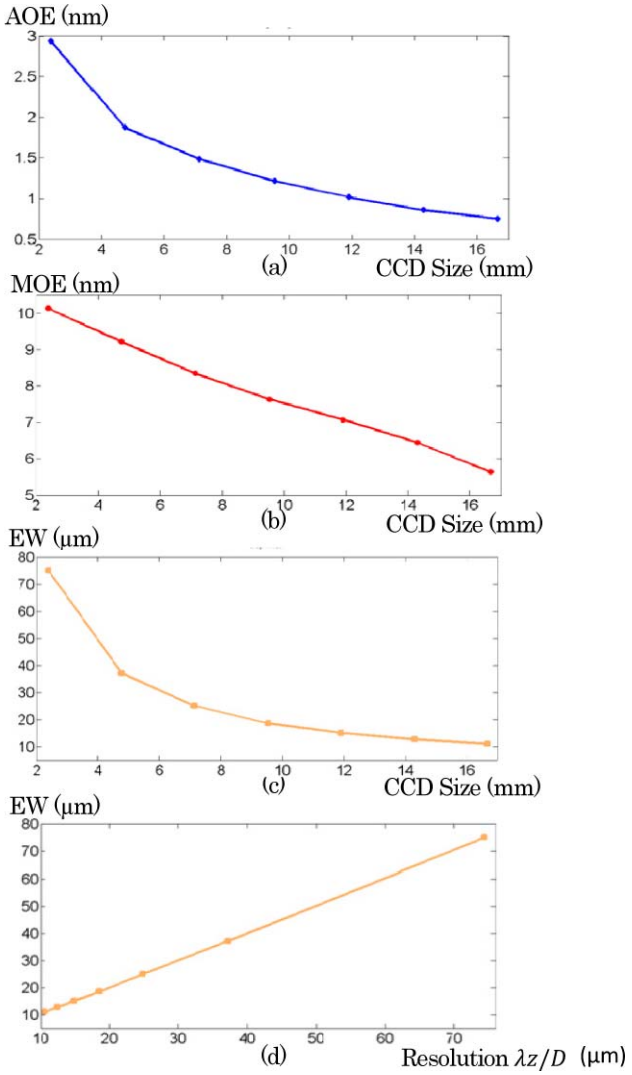

Fig. 2. (Color online) Relationships between (a) AOE, (b) MOE, and (c) EW and CCD size, respectively. (d) Relationship between EW and lateral resolution $\lambda z/D$.

the point of view of information theory, a CCD size of $2D$ causes a bandwidth limit of $2D/\lambda z$ in the spectrum. Therefore a larger CCD size means more object information is recorded. Hence the OPD error is reduced. From the point of view of the PSF in Eq. (4), larger CCD size reduces the spread width and the spread amplitude of the sinc function and therefore reduces the spread width and the amplitude at $x\neq x_0$ of PSF. As the reconstructed image is the weighted sum of the PSFs of all such object points, the accumulated phase errors due to factor $\exp[-(j\pi/\lambda z)(x^2-x_0^2)]$ of Eq. (4) in the reconstructed image are reduced accordingly. Figure 2(c) shows that a larger CCD size increases the measurement accuracy of EW. If we change the x coordinate from CCD size to the lateral resolution, the relation between the measured EW and the lateral resolution is obtained as in Fig. 2(d). It can be seen that the measured EW is nearly equal to the lateral resolution. This is because the infinitely steep edge can only be imaged into a minimum resolvable size due to the lateral resolution of the system. Indeed, the lateral resolution of the DH system is mainly determined by factor $\mathrm{sinc}((2D/\lambda z)x)$ [6]. Therefore, a larger 2D

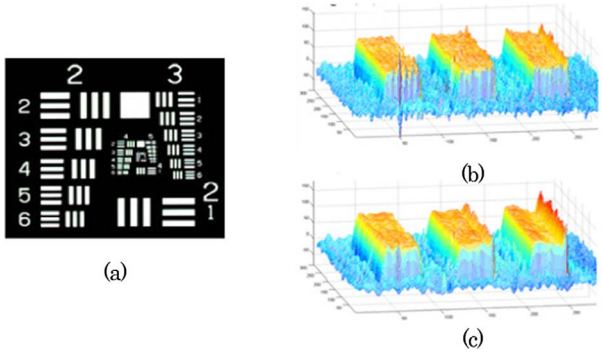

Fig. 3. (Color online) (a) USAF target, (b) G2E3 of the reconstructed 3D image from 960×960 hologram, and (c) G2E3 of the reconstructed 3D image from 660×660 hologram.

provides better lateral resolution and hence increases the measurement accuracy of EW.

The impact of finite CCD size on the axial error is further examined by experiment. In the experiment, seven holograms are recorded with different CCD sizes of 960×960, 910×910, 860×860, 810×810, 760×760, 710×710, and 660×660 pixels, respectively. Each pixel is 4.65 μm × 4.65 μm. A reflective USAF target shown in Fig. 3(a) with 100 nm thin film coated bars was used as the sample.

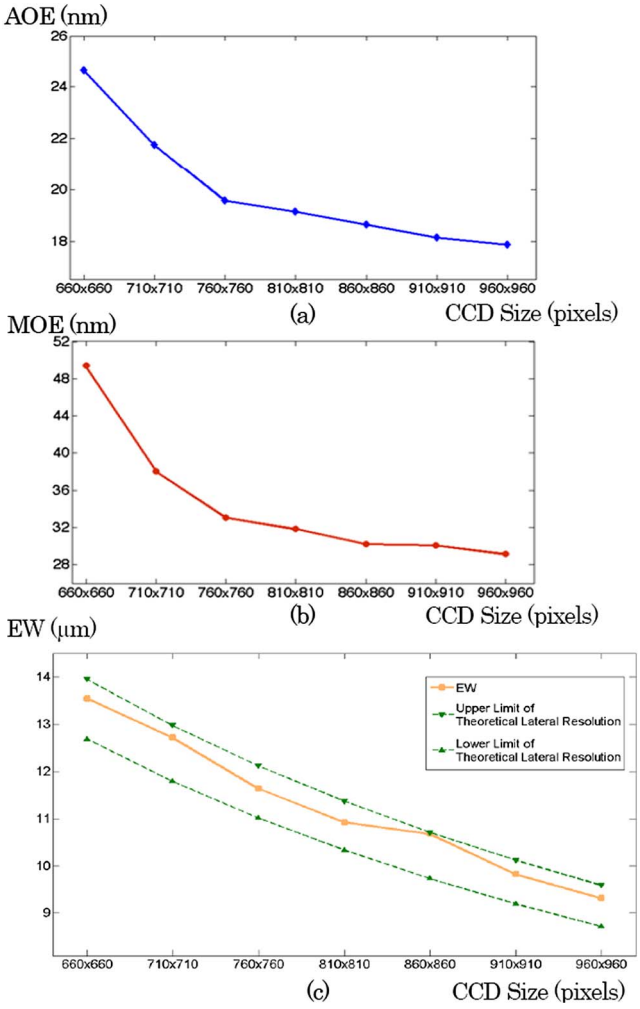

Fig. 4. (Color online) Relationship between (a) AOE, (b) MOE, and (c) EW and CCD size, respectively.

The 3D images are reconstructed from the holograms. As the field of view is different in each reconstruction, a common area group 2 element 3 (G2E3) is used for investigation. 3D profiles of the G2E3 elements reconstructed from holograms of sizes 960×960 and 660×660 are shown in Figs. 3(b) and 3(c). Differences in the axial measurement errors are readily seen. To quantize the differences, the AOE, MOE, and EW of G2E3 at different CCD sizes are evaluated and shown in Fig. 4.

In Figs. 4(a) and 4(b), it is seen that a larger CCD size reduces the AOE and MOE and therefore the axial errors. This result agrees with the simulation investigation in Figs. 2(a) and 2(b). The absolute values of AOE and MOE in Fig. 4 are larger than those in Fig. 2. This is because there are other factors contributing to the axial errors besides the CCD size in experiments. Furthermore, the simulation is performed in one dimension. If two dimensions are considered, the errors are larger. This also explains why the variation ranges of AOE and MOE in Fig. 4 are larger than those in Fig. 2.

The relationship between the EW and CCD size is shown in Fig. 4(c). The solid line shows the measured EW values. The dashed lines show the lateral resolution range. Due to the space variant effect of the DH system, the practical lateral resolution is in the range of $\lambda z/2D$ and $1.1x(\lambda z/2D)$ [6]. Figure 4(c) shows that the measured EW follows the trend of the lateral resolution of the DH system. This result agrees with the result in the simulation and demonstrates that larger CCD size improves the measurement accuracy of edges.

In summary, the impact of CCD size on the axial measurement error is investigated by both simulation investigation and experimental validation. The results show that a larger CCD size can reduce axial error and improve EW measurement accuracy.

I would like to express my gratitude toward Dr. Kemao Qian for his valuable explanation of the phase character in Fourier transform and Dr. Lei Huang for his valuable suggestions in the phase analysis.

References

1. U. Schnars and W. Juptner, Appl. Opt. **33**, 179 (1994).
2. U. Schnars and W. P. O. Juptner, Meas. Sci. Technol. **13**, R85 (2002).
3. N. Pandey and B. Hennelly, Appl. Opt. **50**, B58 (2011).
4. H. Z. Jin, H. Wan, Y. P. Zhang, Y. Li, and P. Z. Qiu, J. Mod. Opt. **55**, 2989 (2008).
5. D. P. Kelly, B. M. Hennelly, N. Pandey, T. J. Naughton, and W. T. Rhodes, Opt. Eng. **48**, 095801 (2009).
6. Y. Hao and A. Asundi, Appl. Opt. **50**, 11 (2011).
7. G. A. Mills and I. Yamaguchi, Appl. Opt. **44**, 1216 (2005).
8. T. Colomb, J. K. Kuhn, F. Charriere, C. Depeursinge, P. Marquet, and N. Aspert, Opt. Express **14**, 4300 (2006).
9. P. Marquet, B. Rappaz, P. J. Magistretti, E. Cuche, Y. Emery, T. Colomb, and C. Depeursinge, Opt. Lett. **30**, 468 (2005).
10. F. Charriere, J. Kuhn, T. Colomb, F. Montfort, E. Cuche, Y. Emery, K. Weible, P. Marquet, and C. Depeursinge, Appl. Opt. **45**, 829 (2006).
11. C. J. Mann, L. F. Yu, C. M. Lo, and M. K. Kim, Opt. Express **13**, 8693 (2005).
12. J. W. Goodman, *Introduction to Fourier Optics*, 2nd ed. (McGraw-Hill, 1996).